

Kinetic models of surface explosions

This article has been downloaded from IOPscience. Please scroll down to see the full text article.

1995 J. Phys.: Condens. Matter 7 6379

(<http://iopscience.iop.org/0953-8984/7/32/005>)

View [the table of contents for this issue](#), or go to the [journal homepage](#) for more

Download details:

IP Address: 171.66.16.151

The article was downloaded on 12/05/2010 at 21:53

Please note that [terms and conditions apply](#).

Kinetic models of surface explosions

R G Sharpe and M Bowker

Department of Chemistry, University of Reading, Whiteknights Park, PO Box 224, Reading RG6 6AD, UK and Interdisciplinary Research Centre in Surface Science, University of Liverpool, PO Box 147, Liverpool L69 3BX, UK

Received 10 March 1995, in final form 24 May 1995

Abstract. The kinetics of surface ‘explosions’ on single-crystal surfaces has been explored by mathematical modelling of a number of possible kinetic models and examining the quality of fit to a wide range of experimental data. Second-order autocatalysis has been the previously preferred model. However, this model is inconsistent since it assumes a random distribution of adsorbates on the surface and yet islanding is known to occur in a number of ‘explosive’ adsorbate systems. Indeed, it is found to be necessary to assume a high *local* coverage (practically independent of the global coverage) near initiation sites to fit the data well. Hence, a new approach that takes into account the effect of interactions between neighbouring adsorbates is required. A circular island model is developed which incorporates the effects of asynchronous initiation and the reduced yield caused by island merging using simple assumptions. This is found to be capable of producing fits to ‘explosive’ desorption data as good as those obtained by the second-order model.

1. Introduction

A number of reactions on a number of single-crystal surfaces are known to occur through surface ‘explosions’ which manifest themselves as anomalously narrow temperature-programmed desorption (TPD) peaks and an autocatalytic increase in desorption rate under isothermal conditions. For instance, the ‘explosive’ decomposition of carboxylate species, leading to narrow CO_2 and H_2 TPD peaks (or H_2O if oxygen is coadsorbed) has been observed on a wide range of surfaces (often in the presence of coadsorbates). These include formate decomposition on Ni(110) [1–4] and Ni(111) [5] and acetate decomposition on Ni(110) [6], Rh(110) (when coadsorbed with C, O or N) [7, 8], Rh(111) (when coadsorbed with K [9] or O [9,10]) and Pd(110) (when coadsorbed with C or O) [11]. The temperature of the desorption peak maximum in these cases is independent of the *global* coverage of the carboxylate species (although no ‘explosion’ is observed at low exposures and the peak temperature and width is very sensitive to the coverage of coadsorbates) [3, 5–11]. Since it is assumed that a high *local* coverage of the decomposing intermediate is required for an ‘explosion’ to occur, this indicates that islanding of carboxylate species occurs in these cases. Further evidence of islanding has been found by sequentially adsorbing DCOOH and HCOOH on Ni(110) [4]. It is found that the ‘explosive’ decomposition of the deuterated formate species has to occur before decomposition of the HCOO species indicating that the initial adsorbates occupy the sites which nucleate island growth and subsequently initiate the reaction. The role of the co-adsorbates is therefore twofold: to induce islanding and to prevent decomposition occurring at temperatures below the ‘explosion’ temperature through other mechanisms by blocking the appropriate surface sites [8]. Thus, on the Rh(111) surface

'explosive' decomposition of acetate can only occur, in the absence of co-adsorbates, if the surface is saturated by acetate [9].

Surface 'explosions' have also been observed in the reaction between NO and CO on Pt(100) leading to narrow N₂, CO₂ and N₂O peaks [12–16]. The temperature of the desorption peak maximum is found to be independent of the ratio of the coverage of the two reactants. However, on the Ru(001) surface, anomalously narrow TPD peaks have been observed where the peak temperature is dependent on the coverage of the intermediate(s) as a result of the desorption of coadsorbed CO and metallic potassium [17]; the desorption of CO₂ following formic acid decomposition [18] and the desorption of hydrogen when oxygen was present in a p(2 × 2) structure [19, 20] (although in this latter case it has also been reported that the desorption is hydrogen coverage independent [21]).

'Explosions' have also been observed due to reactions on a number of non-single-crystal surfaces: the decomposition of formate on a silica-supported nickel catalyst [22], the decomposition of acetate (when oxygen was coadsorbed) on an alumina-supported rhodium catalyst [23] and the reaction between NO and CO on palladium powder [24].

The autocatalytic nature of the desorption has been confirmed, for a number of cases, by the narrow width of the desorption peak observed when the temperature is held constant just below the peak temperature [2, 6, 9, 11, 18, 23]. Strictly, this test is required in all cases to confirm that the desorption is truly 'explosive'.

Two models have been previously proposed to explain 'explosive' kinetics [3]: second-order autocatalysis and the circular island model. The former model assumes, for the case of dissociation of a single adsorbate, that the yield is proportional to both the density of the adsorbed species (and, hence, the coverage, θ) and the density of empty sites (and, hence, $1 - \theta$):

$$-\frac{d\theta}{dt} = k\theta(1 - \theta) \quad (1)$$

where $k = A \exp\{-E_a/RT\}$ is the rate constant, A is the pre-exponential factor, E_a is the activation energy, R is the molar gas constant and T is the absolute temperature. In the circular island model it is assumed that the reaction initiates at certain points on the surface leaving a small circle of free surface sites allowing adsorbate decomposition to occur at the circumference of the circle which therefore grows with time.

The second-order model has been previously found to produce a good fit to the 'explosive' decomposition of formate on Ni(110) provided that the initial coverage was always set to a value close to unity regardless of the real coverage [3]. It has also been used to model the coverage-sensitive narrow CO₂ TPD peaks which result from formate decomposition on Ru(001) provided a coverage-dependent activation energy was used [18] (although, in this case, a first-order desorption model has also been proposed [25]). A second-order autocatalytic step has also been postulated to model the surface 'explosion' that occurs in the reaction between NO and CO on Pt(100) [15] and to explain the kinetic oscillations that occur, under the appropriate conditions, in this reaction and in CO oxidation on Pt(100), Pt(110), Pt(210) and Pd(110) [26, 27].

The circular island model, conversely, was found to produce exceedingly poor fits and thus was dismissed [3]. However, the model used was exceedingly crude and it therefore seems unreasonable to dismiss the concept of island-mediated decomposition simply on this basis. In this paper the model is re-examined taking into account the effects of staggered initiation and island merging.

2. Second-order model

2.1. Modelling

As mentioned above, this model has been used to explain the 'explosive' decomposition of formate on Ni(110) [3] although this was done by including the effect of initiation sites in the coverage of empty sites:

$$-\frac{d\theta}{dt} = k\theta(1 - \theta + f) \quad (2)$$

where f is the proportion of adsorbate sites which are initiation sites and θ is the coverage of non-initiation sites. This can be reduced to equation (1) by setting $f = 0$.

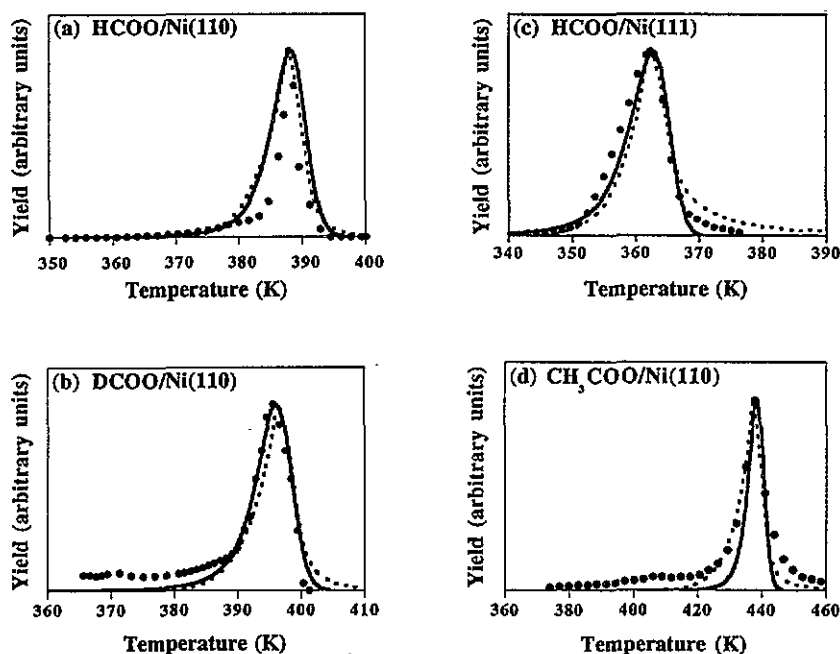


Figure 1. Comparison of the fits obtained by the second-order model (solid line) and new circular island model (dotted line) to TPD data (circular dots) from various 'explosive' adsorbate systems: (a) formate on Ni(110) [1], (b) deuterated formate on Ni(110) [3], (c) formate on Ni(111) [5] and (d) acetate on Ni(110) [6]. The parameters used in the fits are listed in table 1.

Equation (2) can be integrated analytically to give:

$$\theta(t) = (1 + f)\theta_0 / \left[\theta_0 + (1 - \theta_0 + f) \exp \left\{ (1 + f) \int_0^t k dt \right\} \right] \quad (3)$$

and hence the yield as a function of time is given by

$$-\frac{d\theta(t)}{dt} = (1 + f)^2 k \theta_0 (1 - \theta_0 + f) \exp \left\{ (1 + f) \int_0^t k dt \right\} \times \left[\theta_0 + (1 - \theta_0 + f) \exp \left\{ (1 + f) \int_0^t k dt \right\} \right]^{-2} \quad (4)$$

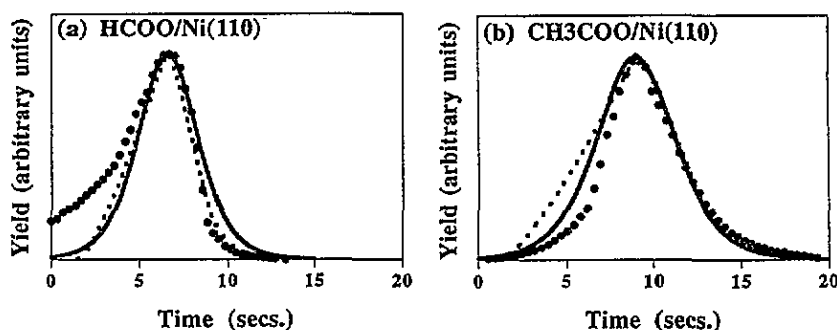


Figure 2. Comparison of the fits obtained by the second-order model (solid line) and new circular island model (dotted line) to isothermal desorption data (circular dots) from various 'explosive' adsorbate systems: (a) formate on Ni(110) [2] and (b) acetate on Ni(110) [6]. The parameters used in the fits are listed in table 1.

For isothermal experiments, where the rate constant is constant throughout, this can be solved analytically and we find that the yield has a maximum of $(1+f)^2 k/4$ at $t = [1/(1+f)k] \ln[\theta_0/(1-\theta_0+f)]$. However, if k is dependent on time, as would be the case in TPD experiments, the yield can be calculated either by numerical integration of the rate constant with respect to time or, alternatively, from equation (2) by an incremental method. In the latter case, the initial coverage, θ_0 , determines the initial yield:

$$-\left(\frac{d\theta}{dt}\right)_0 = k_0\theta_0(1-\theta_0+f)$$

where

$$k_0 = A \exp\left\{-\frac{E_a}{RT_0}\right\}$$

which, in turn, determines the coverage by the next time increment:

$$\theta_1 = \theta_0 - \left(\frac{d\theta}{dt}\right)_0 \Delta t$$

when the temperature becomes $T_1 = T_0 + \beta \Delta t$ where β is the heating rate and so on.

When modelling TPD data an initial temperature, $T_0 = T_{init}$, is arbitrarily chosen to be just below the temperature at which the onset of significant desorption is observed. The effect of the ramp up to this temperature could be incorporated, provided f is sufficiently small, by setting $T_0 = T_{ad}$, the adsorption temperature (and hence the temperature at the start of the ramp) and choosing an initial coverage sufficiently close to unity that the coverage only falls to the initial value used in the modelling by the time the temperature has reached T_{init} . However, since the initial yield must be greater than $k_0 f$, it is found that, for sufficiently large f , the model predicts that all the yield occurs at temperatures well below those seen experimentally using any reasonable values of the pre-exponential factor, A and activation energy, E_a . For instance, if formate decomposition on the Ni(110) surface is modelled using $f = 0.005$ as suggested by Falconer and Madix [3] and $T_0 = 303$ K (the experimental adsorption temperature) the peak temperature is well below the real one with a much larger width. Hence, in this case, it would be necessary to assume that there is an inhibition of initiation at lower temperatures as Fink *et al* [27] did (even with $f = 0$) when modelling the 'explosive' reaction of NO and CO on Pt(100) (they assumed that molecular desorption of NO occurred slowly as the temperature was raised until the coverage fell

Table 1. Experimental results and modelling parameters from 'explosions' of carboxylate species on nickel single-crystal surfaces. In the circular island model a number of parameters were kept fixed throughout at physically meaningful values: $f = 10^{-6}$, $N = 10^{19} \text{ m}^{-2}$, $r_0 = 10 \text{ \AA}$ and $h = 10 \text{ \AA}$.

System	Experimental results				Second-order model parameters				Circular island model parameters		
	Reference	Peak position	Peak width	β (K s^{-1})	E_a (kJ mol^{-1})	θ_0	T_0 (K)	A (s^{-1})	τ (s)	T_0 (K)	A (s^{-1})
HCOO/Ni(110)	[1]	388 K	6.5 K	10	104.6	0.996	342	6.5×10^{15}	0.5	370	7.0×10^{16}
	[2]	6.7 s	4 s	0	104.6	0.997	368	6.2×10^{14}	1.0	368	7.0×10^{16}
DCOO/Ni(110)	[3]	396 K	6.5 K	12	111.3	0.993	360	3.0×10^{15}	0.5	378	3.2×10^{17}
HCOO/Ni(111)	[4]	362 K	8 K	20	101	0.981	322	3.3×10^{15}	0.7	340	42×10^{17}
CH3COO/Ni(110)	[6]	438 K	6 K	9.2	118.1	0.9988	403	6.6×10^{14}	1.3	403	5.0×10^{16}
		19 s	5.2 s	0	118.1	0.999998	403	1.36×10^{15}	1.7	403	1.3×10^{17}

below a critical value when the 'explosion' could proceed). In fact, since $f \ll 1$, the effect of this parameter is much the same as that of θ_0 and thus is essentially a 'free' parameter and we shall set $f = 0$ throughout this paper (hence reducing equation (2) to equation (1)).

2.2. Results and interpretation

Figures 1 and 2 show the best fits obtained by the second-order model (using the parameters listed in table 1) to 'explosions' of carboxylate species on nickel single-crystal surfaces. A good fit between the experimental data and the model is obtained in all cases but only if a value of θ_0 close to unity is used in each case.

However, experimentally, the peak temperatures of the 'explosive' peaks observed are very insensitive to the initial coverage of the carboxylate species [3, 5, 6] while this is not the case for the model. Hence, in order to reconcile this with the modelling, it is necessary to assume that the local coverage near initiation sites is high and largely independent of the global coverage. Indeed, as mentioned above, it is known that, at least for the case of formate on Ni(110), the adsorbate islands on the surface and that the 'explosions' are initiated at the nucleation sites [3]. However, the model assumes the adsorbate is arranged randomly on the surface so that the probability of a given site being occupied is $1 - \theta$, regardless of whether it is adjacent to an occupied site or not. Obviously, evidence of islanding is contrary to this assumption. Various attempts have been made to incorporate the effect of lateral interactions between adsorbed molecules into the second-order model [5, 28] but it is not possible to produce coverage-independent peaks in this way. As the peak temperature of the desorption signal due to 'explosions' in a number of systems is also independent of the coverage of the decomposing intermediate(s) [7-16, 21], this suggests that a model based implicitly on interactions between neighbouring molecules is more appropriate.

Further evidence for this is found from the study of kinetic oscillations on single crystals which have also been modelled using the second-order model. In such systems the surface periodically cycles between a high coverage of one adsorbate and a high coverage of another with the transformation occurring via an autocatalytic reaction which rapidly depletes the surface of the original adsorbate. This brings about the predominance of the alternative adsorbate due to a change in the relative sticking probabilities of the two adsorbates caused by a surface reconstruction (as in CO oxidation on Pt(100) and Pt(110) and the reaction between NO and CO on Pt(100)), faceting (as in CO oxidation on Pt(210)) or the adsorption of subsurface oxygen (as in CO oxidation on Pd(110)) [27]. The whole surface is assumed to oscillate in phase, normally due to coupling through the gas phase. However, the adsorption of one adsorbate on the surface covered by the other adsorbate, which starts the autocatalytic reaction, is assumed to initiate at defects [26] which suggests that the microscopic distribution of adsorbates will be non-uniform. In addition, PEEM measurements have shown that, most noticeably for CO oxidation on Pt(100), the reaction does not take place homogeneously, with advancing wavefronts, spirals and even chaotic patterns being readily observable [27]. This is very clear experimental evidence that, during this particular autocatalytic reaction at least, the probability of reaction occurring in a given site is very dependent on the occupancy of neighbouring sites.

Hence, despite the good fits obtained by the second-order model, an alternative explanation must be sought.

3. Circular island model

3.1. Basic model

Owing to the experimental evidence of islanding, Falconer and Madix [3] proposed the circular island model based on the assumptions that the adsorbates remain static throughout the course of the reaction and that the reaction initiates at specific sites on the surface and then proceeds along the circumference of circles of ever increasing radius centred on these initiation sites. If it is assumed that the initiation sites are distributed homogeneously across the surface, it is possible to associate an area, $1/fN$, with each site where f is the proportion of adsorption sites which are initiation sites and N is the total number of adsorbate sites per unit area on the surface. Hence, if all the sites initiate simultaneously, the total yield is given by

$$-\frac{d\theta}{dt} = \frac{\text{desorbing area per site}}{\text{surface area per site}} = \frac{kh2\pi r(t)}{(1/fN)} = khfN2\pi r(t) \quad (5)$$

where k is the rate constant as above, h is the effective thickness of reaction perimeter at the edge of such a circle and $r(t)$ is the radius of the island of clean surface surrounding an initiation site.

The coverage decreases as the circle grows. In fact, provided that the circle does not overlap with any other, the local coverage in the area associated with a given site is given by

$$\begin{aligned} \theta_{loc} &= 1 & \text{if } t < t' \\ \theta_{loc} &= \theta_{init} & \text{if } t = t' \\ \theta_{loc} &= 1 - \pi f N r^2 & \text{if } t > t' \end{aligned} \quad (6)$$

where t' is the time of initiation. Hence, immediately after initiation, the circle has radius

$$r_0 = \sqrt{(1 - \theta_{init})/\pi f N}. \quad (7)$$

At $t > t'$, substituting (6) into (5) gives

$$-\frac{d\theta_{loc}}{dt} = 2hk\sqrt{\pi f N} \sqrt{1 - \theta_{loc}} \quad (8)$$

which integrates to give the coverage in the area associated with a given site as a function of time:

$$\theta_{loc} = 1 - \pi f N \left[r_0 + h \int_{t'}^t k(t'') dt'' \right]^2 \quad (9)$$

and by comparison to (6) we find the radius of a circle that initiated at time t' :

$$r(t, t') = r_0 + h \int_{t'}^t k(t'') dt'' \quad (10)$$

and either by differentiating (9) or using (5) and (10) we find the yield due to that circle:

$$-\frac{d\theta_{loc}}{dt} = 2\pi f N k h \left[r_0 + h \int_{t'}^t k(t'') dt'' \right]. \quad (11)$$

In the case of an isothermal experiment (when k is independent of time) equations (9)–(11) become

$$\theta_{loc} = 1 - \pi f N [r_0 + hk\{t - t'\}]^2 \quad (12)$$

$$r(t, t') = r_0 + hk\{t - t'\} \quad (13)$$

$$-\frac{d\theta_{loc}}{dt} = 2\pi f N k h [r_0 + h k \{t - t'\}]. \quad (14)$$

Hence, the yield increases linearly with time.

On the other hand, if the temperature is not constant during an experiment, the yield from the circle can be calculated either by numerical integration of the rate constant using equation (11) or by using a similar iterative method to that used in the second-order model. The initial *local* coverage, θ_{loc}^0 , and temperature, T_0 , are set so that the initial yield can be calculated from equation (8):

$$-\left(\frac{d\theta_{loc}}{dt}\right)_0 = 2hK_0\sqrt{\pi f N}\sqrt{1 - \theta_{loc}^0}$$

where

$$k_0 = A \exp\left\{-\frac{E_a}{RT_0}\right\}$$

which is used to calculate the coverage at the next iterative step:

$$\theta_{loc}^1 = \theta_{loc}^0 + \left(\frac{d\theta}{dt}\right)_0 \Delta t$$

when the temperature moves on to $T = \beta \Delta t + T_0$ and so on.

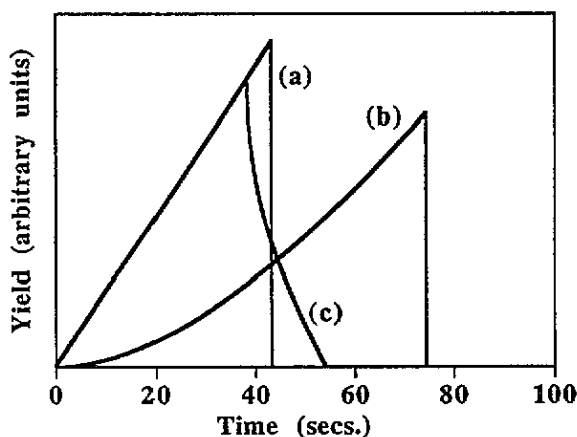


Figure 3. Typical isothermal yield-time relationships derived from various circular island models: (a) the basic model of Falconer and Madix [3] (equation (14)) with $f = 10^{-6}$, $N = 10^{19} \text{ m}^{-2}$, $r_0 = 10 \text{ \AA}$, $h = 10 \text{ \AA}$ and $k = 4 \text{ s}^{-1}$; (b) with the incorporation of staggered initiation only (equation (17)) with $\tau = 50 \text{ s}$ and (c) with the incorporation of island merging only (equation (20)).

When the islands begin to merge the yield can be expected to fall and finally reach zero once all the adsorbate is used up. Previous authors [3, 7] have modelled this by assuming that the yield remains unaffected until the exposed area per initiation site (πr^2) equals the surface area per initiation site ($1/fN$) when it falls to zero. Unsurprisingly, these assumptions have led to yield-time relationships in very poor agreement with experiment (e.g. in the isothermal case the predicted graph is triangular as shown in figure 3(a)) and on this basis the model has been dismissed.

3.2. Beyond the basic model

However, the fit to such simplistic analysis can not be expected to prove or disprove the concept of island growth. In particular, there are a number of assumptions in the above analysis which are clearly unreasonable:

(i) All the initiation sites initiate at the same time.

(ii) The effect of island merging is abrupt (in fact, when two or more circles come into contact the rate of desorption will slow down as the circles overlap but will not fall to zero until all the adsorbate has been exhausted).

(iii) The adsorbate decomposes immediately upon becoming free from its neighbours. It is possible that the adsorbate may diffuse across the circle of free surface sites prior to decomposition at a rate determined by a different rate constant.

(iv) The initiation sites are homogeneously spread across the surface.

(v) The initiation sites are all specific spots on the surface leading to circular growth. Initiation on steps might occur leading to rectangular strips of exposed surface or reaction may occur preferentially in a given direction on the surface as has recently been observed in the reaction between islands of methoxy and oxygen atoms on the Cu (110) surface [29].

We shall attempt to relax some of these assumptions in order to produce a more realistic circular island model.

3.3. Staggered initiation

We shall assume that prior to $t = 0$, initiation is inhibited and that after this the probability that a given initiation site becomes 'active' in the time interval t' to $t' + dt'$ is given by

$$P(t') dt' = \frac{1}{\tau} \exp \left\{ -\frac{t'}{\tau} \right\} dt'. \quad (15)$$

The distribution of initiation probability as a function of time that this predicts is shown in figure 4. It is possible that different initiation probabilities are possible but this assumption is useful as a first attempt at modelling the effect of staggered initiation.

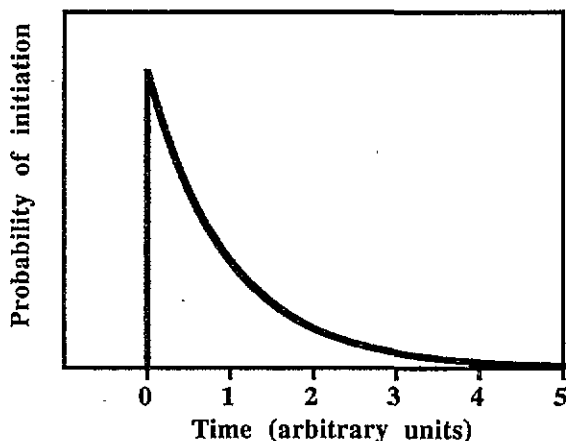


Figure 4. Distribution of initiation probability as a function of time assumed in the circular island modelling.

Hence, the yield per site is

$$-\frac{d\theta}{dt} = \int_0^t [\text{probability of initiating at time } t'] [\text{yield if initiated at time } t'] dt' \\ + [\text{probability of initiating at time } t] [\text{yield if initiating at time } t].$$

The first term is governed by equation (13) but the yield caused by the process of initiation, $fN\pi r_0^2$ per site, is not. Thus

$$-\frac{d\theta}{dt} = \int_0^t \left[\frac{1}{\tau} \exp \left\{ -\frac{t'}{\tau} \right\} dt' \right] \left[2\pi f N h k \left\{ r_0 + h \int_{t'}^t k dt \right\} \right] \\ + \left[\frac{1}{\tau} \exp \left\{ -\frac{t}{\tau} \right\} \right] [fN\pi r_0^2]. \quad (16)$$

If an isothermal experiment is done

$$-\frac{d\theta}{dt} = 2\pi f N h k \int_0^t \frac{1}{\tau} [r_0 + h k \{t - t'\}] \exp \left\{ -\frac{t'}{\tau} \right\} dt' + (fN\pi r_0^2) \frac{1}{\tau} \exp \left\{ -\frac{t}{\tau} \right\} \\ = \frac{\pi f N}{\tau} \left[r_0^2 \exp \left\{ -\frac{t}{\tau} \right\} + 2r_0 h k \tau \left(1 - \exp \left\{ -\frac{t}{\tau} \right\} \right) \right. \\ \left. - 2(hk\tau)^2 \left(1 - \exp \left\{ -\frac{t}{\tau} \right\} - \frac{t}{\tau} \right) \right]. \quad (17)$$

Integrating this gives us the coverage as a function of time:

$$\theta = 1 - \pi f N \left[r_0^2 \left(1 - \exp \left\{ -\frac{t}{\tau} \right\} \right) - 2r_0 h k \tau \left(1 - \exp \left\{ -\frac{t}{\tau} \right\} - \frac{t}{\tau} \right) \right. \\ \left. + 2(hk\tau)^2 \left(1 - \exp \left\{ -\frac{t}{\tau} \right\} - \left(\frac{t}{\tau} \right) + \frac{1}{2} \left(\frac{t}{\tau} \right)^2 \right) \right] \quad (18)$$

(since $\theta = 1$ when $t = 0$ as none of the sites have initiated). The same expression can be calculated geometrically from the area of the average circle:

[area of site][fraction uncovered] = [average circle area]

$$\frac{1}{fN} (1 - \theta) = \int_0^t \frac{1}{\tau} \exp \left\{ -\frac{t'}{\tau} \right\} \pi \{r_0 + h k \{t - t'\}\}^2 dt' \\ \theta = 1 - \pi f N \left[r_0^2 \int_0^t \frac{1}{\tau} \exp \left\{ -\frac{t'}{\tau} \right\} dt' - 2r_0 h k \int_0^t \frac{(t - t')}{\tau} \exp \left\{ -\frac{t'}{\tau} \right\} dt' \right. \\ \left. + (hk)^2 \int_0^t \frac{(t - t')^2}{\tau^2} \exp \left\{ -\frac{t'}{\tau} \right\} dt' \right]$$

which, if the three integrations are performed, yields equation (18) as expected.

This modification to the basic model leads to a more curved yield-time relationship at early times as shown in figure 3(b).

3.4. The effect of island merging

Another way of making the model more realistic is to take into account the decrease in yield of a given circle as it merges with its neighbours. This is difficult to do accurately since, in reality, the initiation sites will be inhomogeneously spaced and will not initiate simultaneously. However, some improvement can be made by splitting the surface into a

series of square cells with side $2a = 1/\sqrt{fN}$ each with an initiation site at its centre (as shown in figure 5) and assuming that the adsorbates inside a given cell are unaffected by the liberation of adsorbates in any neighbouring cell. (In reality these cells are unlikely to be square but it is possible that such cells exist on the surface, perhaps bounded by step edges.) Hence, once the radius of the islands equals half the separation between the initiation sites (i.e., $r = a$) the circumference of the adsorbate is no longer given by $2\pi r$ and equation (5) breaks down. This occurs when the fraction of surface exposed in the cell, $1 - \theta_{loc} = \pi/4$. Figure 5 shows that, at lower coverages, the reaction inside a given cell proceeds along the arcs of radius r subtending an angle ϕ and the effective circumference is reduced from $2\pi r$ to $4r\phi$ where

$$\phi = \frac{\pi}{2} - 2 \cos^{-1} \left(\frac{a}{r} \right). \quad (19)$$

Hence, by reference to equation (5), it is easy to see that the yield would be given by

$$-\frac{d\theta_{loc}}{dt} = khfN4r\phi. \quad (20)$$

The coverage can be calculated geometrically:

$$\begin{aligned} 4a^2(1 - \theta_{loc}) &= 2\phi r^2 + 4a\sqrt{r^2 - a^2} \\ \theta_{loc} &= 1 - \frac{\phi}{2} \left(\frac{r}{a} \right)^2 - \sqrt{\left(\frac{r}{a} \right)^2 - 1}. \end{aligned} \quad (21)$$

Differentiating this equation yields equation (20) as expected since $a = 1/2\sqrt{fN}$,

$$\frac{d\phi}{dt} = \frac{-2a}{r\sqrt{r^2 - a^2}} \frac{dr}{dt}$$

(from equation (19)) and $dr/dt = kh$ (from equation (10)). This modification leads to a more curved yield-time relationship towards the end of the reaction as can be seen in figure 3(c).

3.5. Combining staggered initiation and island merging

We have seen that relaxing the assumption that initiation is synchronous tends to produce a more curved yield-time relationship at high global coverages while relaxing the assumption that islands merge abruptly tends to produce a more curved relationship at low global coverages. Hence, combining the two might give a generally more curved relationship and hence fit the data well. To find the yield at time t we first need to calculate, for each initiation time, $t' < t$, the radius, $r(t, t')$, of islands in sites that initiated at that time, using equation (10). Then, if $r(t, t') < a$, the site yield, $Y(t, t')$, is given by equation (11) while, if $r(t, t') > a$, $Y(t, t')$ is given by equation (20) where ϕ is calculated from equation (19).

The average yield per site is thus given by

$$-\frac{d\theta}{dt} = \int_0^t Y(t, t')P(t') dt'. \quad (22)$$

There is a large number of parameters involved in this model. However, the parameters f and N , and h and A , always occur as products and the activation energy, E_a , is determined experimentally for the data modelled in this paper. This leaves only four degrees of freedom in choosing the initial radius, r_0 , the time constant, τ , as well as the products fN and hA . In practise, the values of f , N , r_0 and h are kept fixed at physically meaningful quantities and only A and τ were adjusted to achieve the fits.

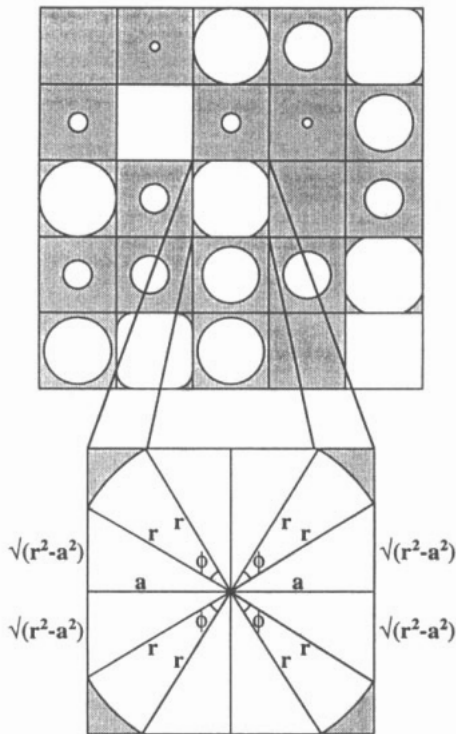


Figure 5. Schematic of the geometry of island merging when initiation is staggered and initiation sites are homogeneously spaced. The shaded area is covered by adsorbate while the white areas are adsorbate free. One cell in which the circular island growth has been curtailed by the edge of the cell has been exploded. The area of clean surface in this cell can be calculated by summing the area of the four segments (each of area $\frac{1}{2}\phi r^2$) and the eight triangles (each of area $\frac{1}{2}r\sqrt{r^2 - a^2}$).

3.6. Results and interpretation

Figures 1 and 2 also show the best fits obtained by this modified circular island model to 'explosions' of carboxylate species on nickel single-crystal surfaces (the same data as used to test the second-order model) using the values of the parameters listed in table 1. By comparison to the fits obtained using the second-order model, it is clear that, despite the crude assumptions that have been made, the model is capable of fitting the data similarly well. This, of course, does not mean that the model is correct as the values of the parameters involved have been chosen for this purpose but it does demonstrate that the previous rejection of the circular island model on the basis of its inability to produce good fits is unfounded. Slight differences in the shape of the peak could be produced by making different assumptions on the nature of initiation and island merging than those made here.

The growth of circular islands of free sites implies that the diffusion of adsorbates is slow compared to the rate of growth of islands or that, if an adsorbate molecule does free itself from its neighbours so that it diffuses into the circle of free sites, it quickly decomposes. Thus, a further modification to this model would be to allow the circle to have a coverage θ' , of adsorbates which have diffused into it and which decompose at a

rate determined by the second-order model:

$$-\frac{d\theta'}{dr} = k\theta'(1 - \theta')$$

The data can be successfully fitted using such a model but it is found that the large number of parameters allows a good fit to be obtained using widely different parameter values. For instance, the two limiting cases: decomposition inside the circle being rate determining (in which case the yield is determined by the second-order model) and circular island growth being rate determining (in which case the yield is determined by the circular island model derived above) are, as we have seen, both capable of fitting the data well.

4. Conclusions

The second-order autocatalytic model is the one normally used to explain the kinetics of 'explosive' systems. However, a variety of experimental evidence shows that, in such systems, islanding occurs, which is inconsistent with the implicit assumption of the model. We have proposed a circular island model in which the initiation of sites is not synchronous and the effect of island merging is taken into account. This model has fitted the data well using reasonable values of the parameters involved. Hence, the reason for the previous rejection of this model (on the basis of a poor fit between experiment and theory) has been removed. This model is mathematically more complex than the second-order model but is more consistent with experimental evidence. Further refinements to the model proposed here are possible—in particular the assumption that the sites are homogeneously spaced in a square lattice is too simplistic.

References

- [1] McCarty J, Falconer J and Madix R J 1973 *J. Catal.* **30** 235
- [2] Falconer J L, McCarty J G and Madix R J 1974 *Surf. Sci.* **42** 329
- [3] Falconer J L and Madix R J 1974 *Surf. Sci.* **46** 473
- [4] The formate was created by the adsorption of formic acid. In the initial papers [1–3], it was thought that the adsorbate was formic anhydride but further work, using EELS, revealed that this was not the case: Madix R J, Gland J L, Mitchell G E and Sexton B A 1983 *Surf. Sci.* **125** 481
- [5] Benziger J B and Schoofs G R 1984 *J. Phys. Chem.* **88** 4439
- [6] Madix R J, Falconer J L and Suszo A M 1976 *Surf. Sci.* **54** 6
- [7] Bowker M and Li Y 1991 *Catal. Lett.* **10** 249
- [8] Li Y and Bowker M 1993 *J. Catal.* **142** 630
- [9] Hoogers G, Papageorgopoulos D C, Ge Q and King D A 1995 *Surf. Sci.* submitted
- [10] Li Y and Bowker M 1993 *Surf. Sci.* **285** 219
- [11] Aas N and Bowker M 1993 *J. Chem. Soc. Faraday Trans.* **89** 1249
- [12] Fischer T E and Keleman B R 1978 *J. Catal.* **53** 24
- [13] Banholzer W F and Masel R I 1984 *Surf. Sci.* **137** 339
- [14] Lesley M W and Schmidt L D 1985 *Surf. Sci.* **155** 215
- [15] Fink Th, Dath J-P, Bassett M R, Imbühl R and Ertl G 1991 *Surf. Sci.* **245** 96
- [16] Zagatta G, Müller H, Wehmeyer O, Brandt M, Böwering N and Heinzmann U 1994 *Surf. Sci.* **307–309** 199
- [17] Hoffman F M, Hrbek J and Depaola R A 1984 *Chem. Phys. Lett.* **106** 83
- [18] Sun Y-K and Weinberg W H 1991 *J. Chem. Phys.* **94** 4587
- [19] Hrbek J 1986 *J. Catal.* **100** 523
- [20] Hrbek J 1986 *J. Phys. Chem.* **90** 6217
- [21] Anton A B, Parmeter J E and Weinberg W H 1986 *J. Am. Chem. Soc.* **108** 1823
- [22] Falconer J L, Burger L C, Corfa I P and Wilson K G 1987 *J. Catal.* **104** 104
- [23] Cassidy T J, Allen M D, Li Y and Bowker M 1993 *Catal. Lett.* **21** 321
- [24] Moriki S, Inoue Y, Miyazaki E and Yasumori I 1982 *J. Chem. Soc. Faraday Trans.* **78** 171

- [25] Meng B, Jachimowski T A, Sun Y and Weinberg W H 1994 *Surf. Sci. Lett.* **315** L959
- [26] Ertl G 1990 *Adv. Catal.* **37** 213
- [27] Fink Th, Dath J-P, Imbihl R and Ertl G 1991 *J. Chem. Phys.* **95** 2109
Hopkinson A and King D A 1993 *Faraday Discuss.* **96** 255
- [28] Paul A, Jenks C J and Bent B E 1992 *Surf. Sci.* **261** 233
- [29] Leibsle F M, Francis S M, Davis R, Xiang N, Haq S and Bowker M 1994 *Phys. Rev. Lett.* **72** 2569